ELSEVIER

Polymer 42 (2001) 3067–3075

polymer

www.elsevier.nl/locate/polymer

Effect of molecular structure distribution on melting and crystallization behavior of 1-butene/ethylene copolymers

M. Zhang, D.T. Lynch, S.E. Wanke*

Department of Chemical and Materials Engineering, University of Alberta, Edmonton, Alta., Canada T6G 2G6

Received 27 March 2000; received in revised form 30 August 2000; accepted 31 August 2000

Abstract

Short chain branching (SCB) and methylene sequence length (MSL) distributions were measured by TREF and DSC coupled with successive nucleation/annealing (SNA) for a Ziegler–Natta and a metallocene ethylene–butene copolymer. TREF analysis indicated that the copolymer made with Ziegler–Natta catalyst exhibited a broad bimodal SCB distribution, while the polymer made with the metallocene catalysts had a narrow SCB distribution. SNA-DSC analysis showed that the Ziegler–Natta copolymer had a broad MSL distribution with significant amount of long methylene sequences; the metallocene copolymer had a much narrower MSL distribution and contained a large amount of polymer with short methylene sequences. The melting and crystallization measurements on PTREF fractions of the two polymers showed that the melting temperature, crystallization temperature and enthalpy of fusion of the PTREF fractions for the Ziegler–Natta polymer decreased substantially with increasing SCB content, while these properties varied only slightly for the PTREF fractions of the metallocene polymer. This indicates that the SCB distribution has a more significant effect on melting and crystallization behaviors of polyethylene copolymers than the average SCB content.

Keywords: Compositional heterogeneity; Melting and crystallization; Ziegler–Natta and metallocene catalyst

1. Introduction

Copolymers of ethylene and α-olefins are known to have a very heterogeneous chain microstructure with respect to molar mass and short chain branching (SCB). Although molar mass is of importance, the amount and distribution of the SCB are dominant factors for determining the physical properties of ethylene/α-olefin copolymers. These molecular parameters of such copolymers depend in turn on catalysts used for the copolymerization, and can differ considerably from one grade of copolymer to another. Therefore, studies on the effect of molecular structure on the physical properties of ethylene/α-olefin copolymers are of great importance.

Investigation into the relationship between structure and properties of olefin copolymers requires, among other factors, analysis of crystallization and melting behavior. A number of studies have been devoted to the melting and crystallization of homogeneous copolymers of ethylene and α-olefins made with vanadium-based catalysts [1–4] and copolymers made with Ziegler–Natta catalysts [5–7]. The consensus of these studies is that melting and crystallization temperatures of ethylene/α-olefin copolymers decrease considerably with increasing amounts of SCB. The effect of molar mass on melting and crystallization behaviors was found to be small [3,4,8]. It has also been recognized that the melting and crystallization behaviors of ethylene/α-olefin copolymers are complex due to the variations of SCB distributions in the different types of these copolymers. This is even true for homogeneous copolymers of ethylene and 1-octene synthesized using a vanadium-based Ziegler–Natta catalyst; the SCB distribution for these polymers was considered to be uniform [2–4]. This complexity is largely due to the interrelation of SCB, MSL and molar mass distributions, and this interrelation makes it difficult to independently investigate the effect of the different molecular parameters on the crystallization and melting characteristics.

Insight into the crystallization and melting behaviors of commercial ethylene/α-olefin copolymers can be obtained by studying the whole polymer and its compositional fractions. The whole polymer sample can be fractionated according to molecular parameters such as molar mass or SCB, and the crystallization and melting characteristics of the individual fractions, for which the distributions of the structural parameters are narrow, can be studied. Several authors have employed fractionation methods to investigate

* Corresponding author. Tel.: +1-780-492-3817; fax: +1-780-492-2881.
E-mail address: sieg.wanke@ualberta.ca (S.E. Wanke).

0032-3861/01/$ - see front matter
PII: S0032-3861(00)00667-4

Table 1
Properties of the Ziegler–Natta and metallocene copolymers studied

Copolymer	Manufacturer	SCB Content[a](CH_3/1000 C)	Density	M_n[b] $\times 10^{-4}$	Pd[c]
Metallocene	Exxon	32.4	0.880	5.1	2.14
Ziegler–Natta	NOVA	17.7	0.918	3.2	3.28

[a] Obtained from ATREF analysis by method described in Ref. [10].
[b] Number average molar mass.
[c] Polydispersity (M_w/M_n).

structural and crystallization behaviors of ethylene/α-olefin copolymers made with heterogeneous Ziegler–Natta catalysts [5–7,9], and they concluded that these fractionation techniques are effective for exploring the relationships between the structure, and crystallization and melting characteristics of such copolymers.

In the current study, analytical and preparative temperature rising elution fractionation (ATREF and PTREF) and thermally fractionated DSC were used to investigate the molecular structure of two commercial 1-butene/ethylene copolymers. The two polymers were fractionated by PTREF, which yielded a series of samples with similar SCB content but different SCBD. The effect of SCB distributions on the melting and crystallization behavior of the PTREF fractions and the whole polymers were studied using DSC.

2. Experimental

The polyethylenes used in this study were two commercial 1-butene/ethylene copolymers; one made with a Ziegler–Natta catalyst and the other with a metallocene catalyst. The properties of the two polymers are given in Table 1. The polymers will be referred to as Ziegler–Natta copolymer and metallocene copolymer.

Fractionation of the copolymer resins was accomplished by temperature rising elution fractionation (TREF). The polymer samples in *o*-xylene at concentrations of 0.005–0.04 g PE/ml, along with about 1.5 g of glass beads (80–100 mesh), were heated at 125°C for 4 h. The solution and glass beads were then cooled slowly from 125°C to −8°C at a rate of 1.5°C/h in order to crystallize the polymer out of solution onto the glass beads. The crystallized sample was filtered into a stainless steel TREF column which was then connected to the TREF system. A DuPont Instrument 860 Chromatographic pump was used to pump the solvent (*o*-dichlorobenzene) through the TREF column at a rate of 1.0 ml/min, and an on-line IR detector tuned at 2860 cm^{-1} was used to detect the polymer species eluting from the column. Elution was started at 0°C for both ATREF and PTREF.

For ATREF analysis, about 5 mg of polymer was used, and the column temperature was increased at a heating rate of 1°C/min while the solvent was pumped through the column. In the case of PTREF, a sample size of 300 mg was used for the Ziegler–Natta copolymer and 85 mg was used for the metallocene copolymer. For PTREF, the column temperature was raised in 10 min periods from a lower to a higher temperature for each interval and maintained at the high temperature for another 10 min without solvent flowing, then the solvent flow was started at a flow rate of 1.0 ml/min to allow the dissolved polymer to elute from the column. The polymer concentration in the effluent was monitored by the on-line IR detector and the effluent was collected for 10 min. This time was sufficient for collecting all the dissolved polymer at each temperature interval since the IR signal always had returned to the baseline at the end of the 10-min collection period.

The polymer in the PTREF fractions, collected by the procedure described above, was precipitated from the *o*-dichlorobenzene by the addition of 15 ml of acetone. The slurry was filtered using a 0.5 μm Teflon film. The obtained polymer was washed with acetone and dried at ambient temperature. The resulting polymer samples were weighed (size was 5–6 mg) and encapsulated in aluminum pans for subsequent DSC analysis.

The successive nucleation/annealing (SNA) procedure used for the treatment of the whole polymer samples involved a series of heating–annealing–cooling cycles. To erase previous thermal history, the sample was heated at a rate of 5°C/min to 155°C for the Ziegler–Natta sample and to 135°C for the metallocene sample and maintained at that temperature for 1 h. The samples were subsequently cooled to 25°C at a cooling rate of 5°C/min to create the initial "standard" state. Prior experiments with the Ziegler–Natta copolymer showed that initial annealing at 165°C gave the same results as annealing at 155°C. The lower temperature was used to decrease the chance of polymer degradation.

The SNA procedure used for the thermal treatment of the polymer samples was similar to that used in a previous study [10]. The polymer samples were heated at 5°C/min to a selected temperature and maintained at that temperature for 20 min. This step results in partial melting and annealing of polymer crystals. The crystallization was achieved by subsequently cooling the sample to 25°C at a rate of 5°C/min. The heating–annealing–cooling cycle was repeated at a temperature interval of 5°C from 135 to 25°C for the Ziegler–Natta sample and from 105 to 25°C for the metallocene sample.

The DSC endotherms of the samples were measured using a TA Instrument Model DSC2910. An indium

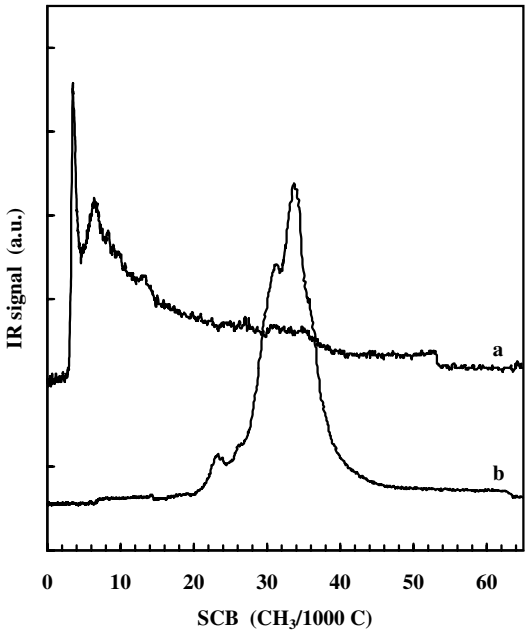

Fig. 1. SCB distribution obtained from ATREF for: (a) Ziegler–Natta copolymer and (b) metallocene copolymer.

standard was used to calibrate the instrument. The SNA-treated whole polymer samples and PTREF fractions (about 6 mg) were heated from 0°C at a heating rate of 10°C/min to 160°C and subsequently cooled to 0°C at the same rate. The melting temperature, crystallization temperature, and enthalpy of fusion were analyzed using the TA2200 software package.

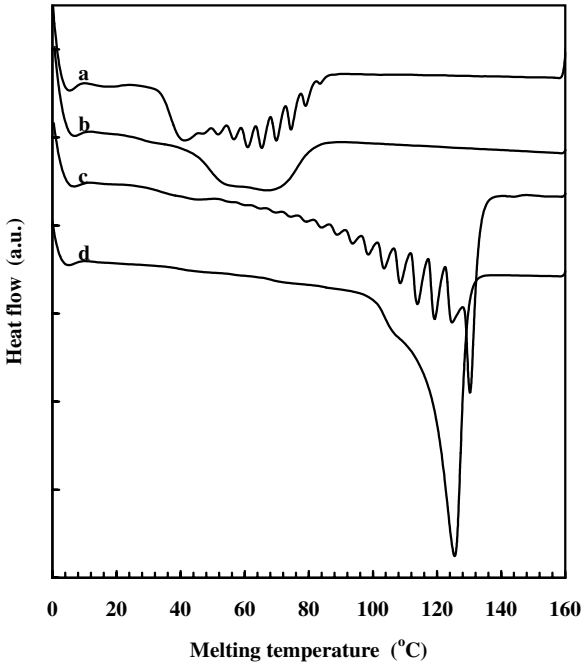

Fig. 2. Comparison of DSC endotherms of different polymers: (a) SNA-treated and (b) as-received metallocene copolymer; (c) SNA-treated and (d) as-received Ziegler–Natta copolymer.

3. Results and discussion

3.1. Molecular structural distribution of Ziegler–Natta and metallocene copolymers

The SCB content is a dominant factor affecting the spherulitic texture and the lamellar morphology, and hence the melting and crystallization behaviors of ethylene/α-olefin copolymers [3–9]; the influence of molar mass is much less significant. As suggested by Peeters et al. [3,4], based on the results with homogeneous copolymers of ethylene and 1-octene synthesized using vanadium-based Ziegler–Natta catalyst, melting and crystallization temperatures of these copolymers declined considerably with increasing SCB content, whereas no clear influence of molar mass was detected. Alamo et al. [8] have shown that the influence of molar mass on melting temperature is much less significant for random ethylene/α-olefin copolymers than comonomer content, especially when the branch content is higher than 2.6 mol%. The molar masses of the samples used in the current study are above the value at which molar mass has an effect on melting and crystallization behaviors, and the SCB concentration for both copolymers is high; hence, this study focuses on the effects of compositional structure on the melting and crystallization behavior.

The compositional distribution of the whole polymer is expressed in two ways: one, the SCB distribution obtained from the ATREF profile by transforming ATREF elution temperature into SCB content using a calibration generated from the TREF-SEC cross-fractionation of a broadly distributed linear polyethylene [10]; and two, the MSL distribution obtained from SNA-DSC endotherms where the melting temperature was transformed into MSL by using a calibration generated from standard hydrocarbons.

Fig. 1 shows the SCB distributions of the Ziegler–Natta and metallocene copolymers generated by ATREF. The Ziegler–Natta sample showed the characteristic bimodal SCB distribution with SCB concentration in the range from 4 to 55 branches per 1000 carbons for the copolymer fraction and the sharp peak with a SCB content of less than 4 branches per 1000 carbons for the 'homopolymer' peak common for 1-butene/ethylene copolymers made with Ziegler–Natta catalysts. The SCB distribution for the metallocene copolymer had a much narrower SCB distribution (16–50 branches per 1000 carbons).

Fig. 2 shows DSC endotherms for the Ziegler–Natta and metallocene copolymers with different thermal histories. The DSC endotherms for the as-received samples (curves b and d in Fig. 2) show significant differences in melting temperatures between the Ziegler–Natta and metallocene copolymer, but they did not provide much information about lamellar thickness or MSL distribution since a polymer crystallized under uncontrolled conditions may undergo melting–recrystallization–remelting during heating [11]. In contrast, the treatment of the copolymer samples

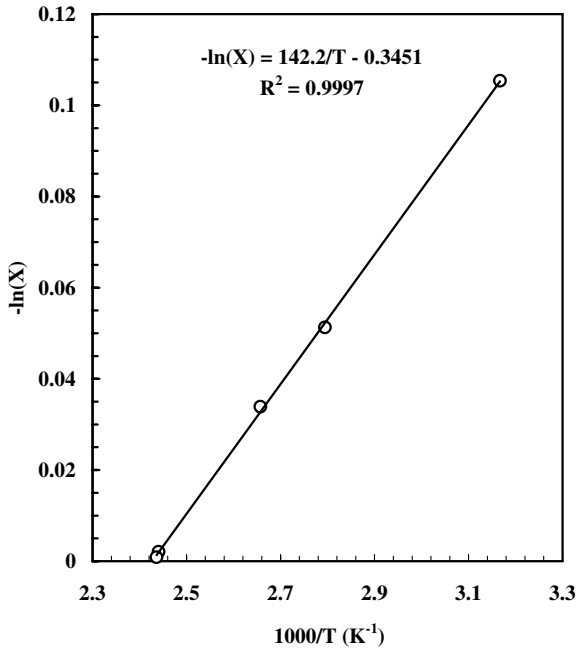

Fig. 3. SNA-DSC calibration curve of mole fraction of CH_2 in polymer as a function of melting temperature.

by the successive nucleation/annealing (SNA) procedure resulted in DSC endotherms with significant segregation (curves a and c in Fig. 2). Essentially, the SNA-DSC, like other thermal treatment procedures [12–15], segregates semicrystalline polymer according to lamellar thicknesses of polymer crystals, or by methylene sequence length (MSL) when the MSL is less than the critical value for chain folding [10,16–19]. As such, each peak of the SNA-DSC endotherm represents a group of chain segments of similar lamellar thickness or MSL. It can be seen from Fig. 2 that the SNA-DSC endotherm of the Ziegler–Natta copolymer exhibited a multiple-peaked distribution at temperatures ranging from 40 to 130°C, indicating that there is a broad distribution of lamellar thicknesses or MSLs.

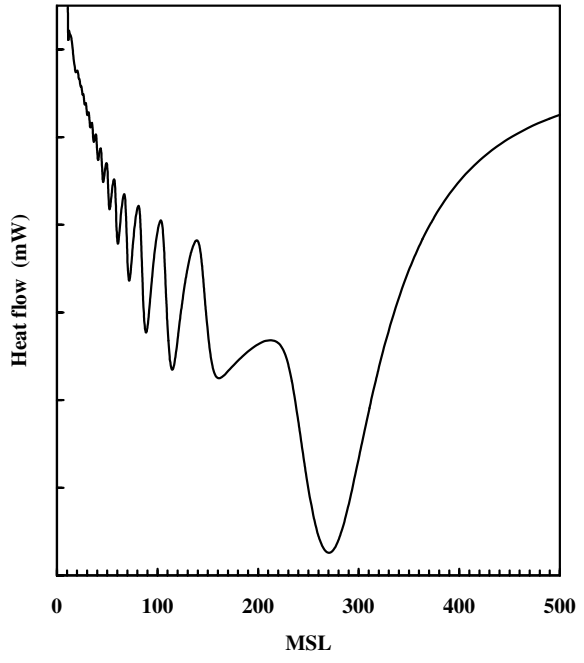

Fig. 4. Methylene sequence length distribution of Ziegler–Natta copolymer obtained from SNA-DSC.

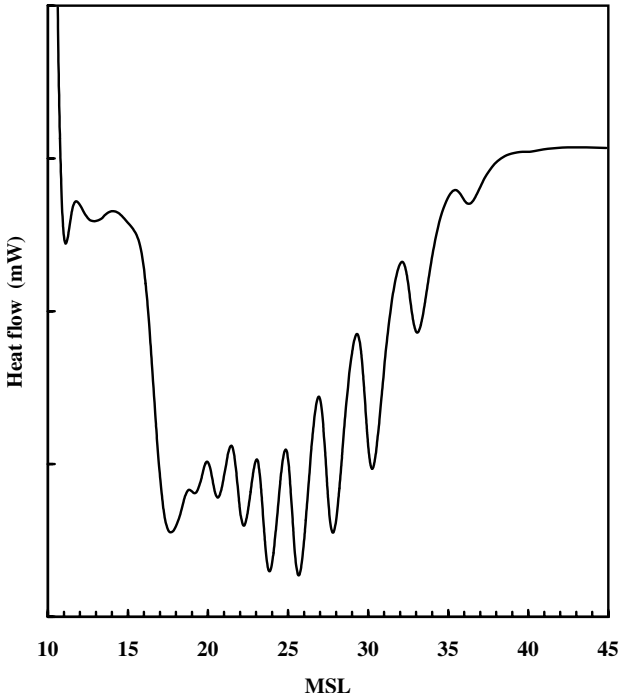

Fig. 5. Methylene sequence length distribution of metallocene copolymer obtained from SNA-DSC.

As shown in Fig. 2, a multiple-peaked DSC endotherm was also observed for the metallocene copolymer pretreated with the SNA procedure, indicating the heterogeneity of the MSL distribution. The metallocene sample had a much narrower MSL distribution, endotherm minima ranging from 40 to 85°C, compared with the Ziegler–Natta copolymer, endotherm minima ranging from 40 to 130°C. It is also of interest to note that the metallocene copolymer, after the SNA treatment, showed a large peak with a minimum at about 40°C. The existence of this peak was fairly reproducible in repeated experiments. This low temperature peak represents chain segments having short MSL, and the area under this low-temperature peak suggests that the metallocene copolymer had an appreciable amount of such short methylene sequences. It seems that these short methylene sequences only crystallized and melted at the low temperatures during the SNA treatment, and were not detected by ATREF nor by a stepwise thermal treatment procedure [20–21]. According to Peeters et al. [4] and Alizadeh et al. [11], short sequences most likely result in metastable fringed micellar-type crystals and can exert different influence on melting and crystallization of copolymers.

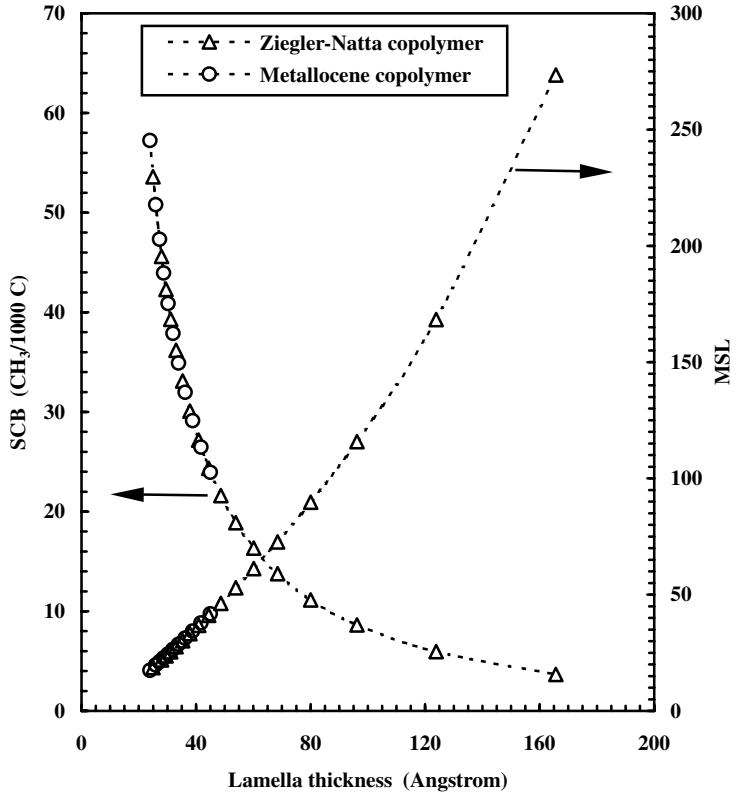

Fig. 6. Relationships between lamella thickness and short chain branches (SCB) and methylene sequence length (MSL) for ethylene–butene copolymers.

To further illustrate the MSL distribution of the Ziegler–Natta and metallocene copolymers, the SNA-DSC endotherms were transformed into MSL distribution curves by using a calibration curve generated from standard hydrocarbons. In the present study, three linear paraffins (C_{20}, C_{40}, and C_{60}) and two standard ethylene homopolymers from the National Institute of Standards and Technology (LP1482 and LP1483) were treated by the SNA as described above, and the melting temperature of each sample was subsequently measured by DSC. The composition and melting temperature were fitted in a manner similar to the one used by Keating et al. [16]. As shown in Fig. 3, the CH_2 mole fraction, X, is well correlated with the melting temperature. It should be pointed out that the crystallization of branched polyethylene chain segments may differ from that of linear paraffins. However, in the absence of better standard samples, the use of linear paraffins as references appears to provide reasonable results in many cases [3,16,22].

The melting temperatures from the SNA-DSC endotherms in Fig. 2 were transformed into MSL by using the calibration curve in Fig. 3. In Figs. 4 and 5 the heat flow is shown as a function of MSL for the Ziegler–Natta and metallocene copolymers. Very different MSL distributions were obtained for the Ziegler–Natta and metallocene copolymers (cf. Figs. 4 and 5). The Ziegler–Natta sample had a broad MSL distribution ranging from 20 to 270 carbons, and a considerable number of chain segments had long sequences of about 270 carbons. This value is below or close to the critical value for the onset of chain folding [17,18], suggesting that MSL-controlled chain crystals would be dominant for the Ziegler–Natta copolymer. This conclusion agrees well with that of Bonner et al. [19]. The metallocene sample had a much narrower MSL distribution in the MSLs in the range of 18–37 carbons, i.e. the MSL distribution for the metallocene copolymer was essentially uniform. Note the above-mentioned peak at a melting temperature of 40°C corresponds to a MSL of about 18 carbons.

3.2. Relation between lamellar thickness and SCB or MSL

As shown above, the SNA-DSC effectively segregated molecular segments according to their lamellar thicknesses, and the use of the calibration (Fig. 3) yielded reasonably good estimates of MSL, and hence the SCB concentration at each melting temperature. Therefore, it is possible to quantitatively determine the relationship between lamellar thickness and SCB or MSL.

The relationship between melting temperature and lamellar thickness is usually described by the Thomson–Gibbs equation [23]:

$$T_m = T_m^o\left(1 - \frac{2\sigma_e}{\Delta H_u L}\right) \quad (1)$$

where T_m is the observed melting temperature (K) of lamella

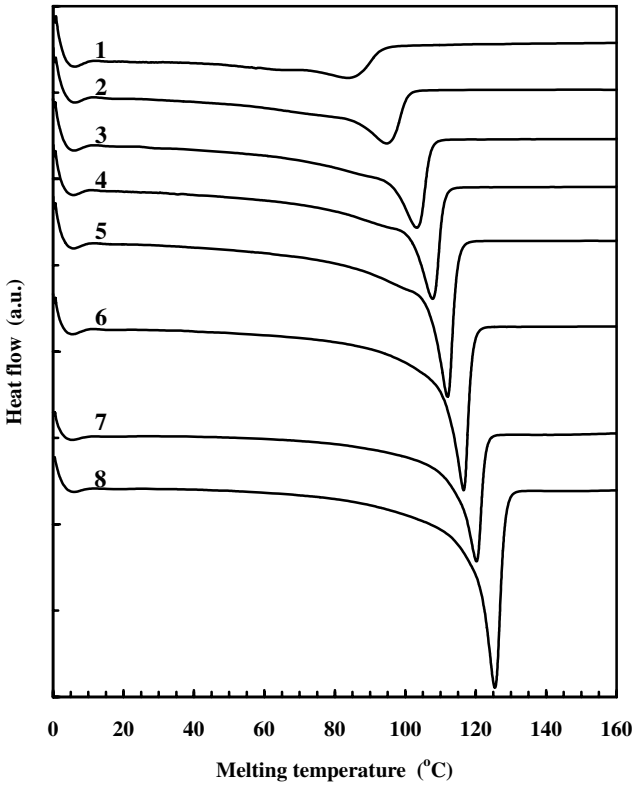

Fig. 7. Evolution of melting behavior for PTREF fractions for Ziegler–Natta copolymer obtained at different fractionation temperatures: (1) 40; (2) 55; (3) 65; (4) 72.5; (5) 77.5; (6) 82.5; (7) 87.5; and (8) 95°C.

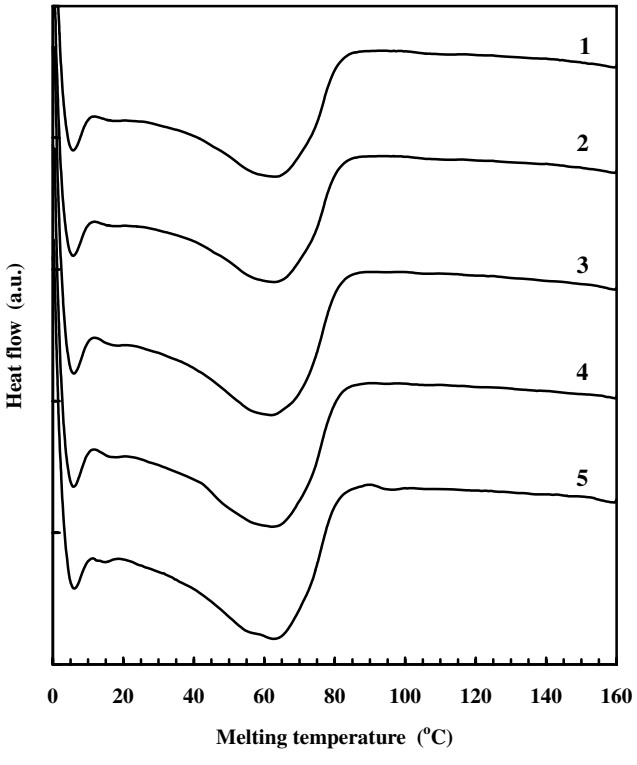

Fig. 8. Evolution of melting behavior for PTREF fractions for metallocene copolymer obtained at different fractionation temperatures: (1) 35; (2) 42.5; (3) 47.5; (4) 52.5; and (5) 60°C.

of thickness L; T_m^o the equilibrium melting temperature of an infinite crystal ($T_m^o = 418.7$ K); σ_e the surface energy per unit area of the basal face ($\sigma_e = 87 \times 10^{-3}$ J/m^2), and is associated with the energy of chain folding during crystallization; and ΔH_u is the enthalpy of fusion for crystalline phase ($\Delta H_u = 290 \times 10^6$ J/m^3) [23,24].

The relationships between lamellar thickness and short chain branches as well as MSL were calculated for the two copolymers based on Eq. (1) and the calibration curve in Fig. 3. The melting temperatures, taken from the peak temperatures of the SNA-DSC endotherms, were used to calculate lamellar thickness and MSL. In Fig. 6, the calculated lamellar thickness is plotted as a function of SCB and MSL. It can be seen that the lamellar thickness increased markedly with decreasing SCB concentration in the low SCB range (less than 15 SCBs/1000 carbons). When the SCB content was more than 15 SCBs/1000 carbons, the lamellar thickness only gradually decreased with increasing SCBs. Also shown in Fig. 6, the lamellar thickness increased with increasing MSL; this suggests that the MSL-controlled chain crystals are dominant for these copolymers. These results are in agreement with results obtained by small angle X-ray scattering on copolymer made with a Ziegler–Natta catalyst [25].

3.3. Melting and crystallization properties of Ziegler–Natta and metallocene copolymers

Polyethylene copolymers can be intramolecularly and intermolecularly heterogeneous in terms of SCB or MSL distribution [9,11,26]. In principle, TREF separates semicrystalline macromolecules according to the crystallizability or average SCB content [27,28]. As a result, molecules in each PTREF fraction collected in a narrow temperature interval can essentially be considered to have the same SCB distribution, and hence the same average SCB content. As a result, the use of PTREF, to a large extent, eliminates the effect of intermolecular heterogeneity of SCBs on the melting and crystallization of copolymer in a PTREF fraction.

The Ziegler–Natta copolymer was fractionated into eight fractions by PTREF. The DSC endotherms of these PTREF fractions are shown in Fig. 7. It can be seen that the melting curve of each PTREF fractions was characterized by a single DSC melting peak with a long tail toward low melting temperatures. As PTREF elution temperature increased, the melting peak became sharper and the melting curve appreciably shifted toward high temperature. These results indicate that the increase in SCB content considerably diminished the melting temperature of the Ziegler–Natta copolymer.

The metallocene copolymer was fractionated into five fractions in the whole ATREF elution temperature range; the PTREF fractions below 35°C contained insufficient polymer for the preparation of DSC specimen. The DSC endotherms of these PTREF fractions are shown in Fig. 8.

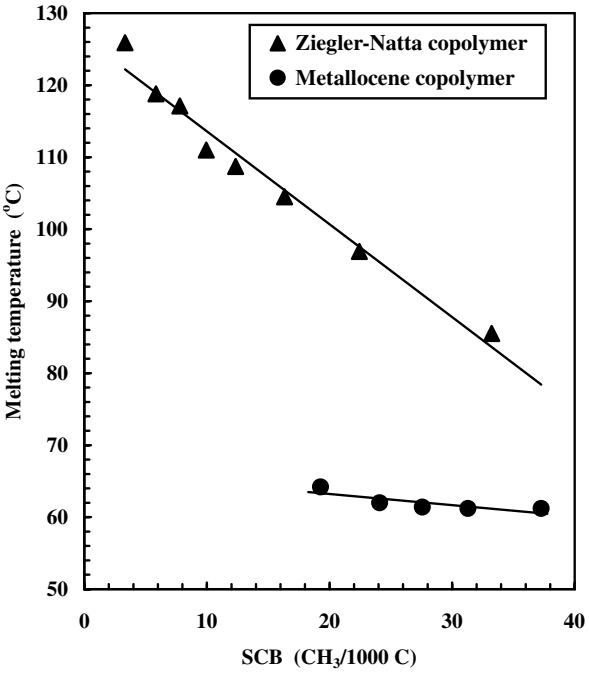

Fig. 9. Dependence of melting peak temperature on SCB content for Ziegler–Natta and metallocene copolymers.

A single, broad, and unsymmetrical peak was observed for each fraction. Unlike the PTREF fractions of the Ziegler–Natta copolymer, those of the metallocene sample showed little change in the melting curves with increasing PTREF elution temperature, suggesting that the decrease in SCB content has little effect on the melting of the PTREF fractions of the metallocene copolymer.

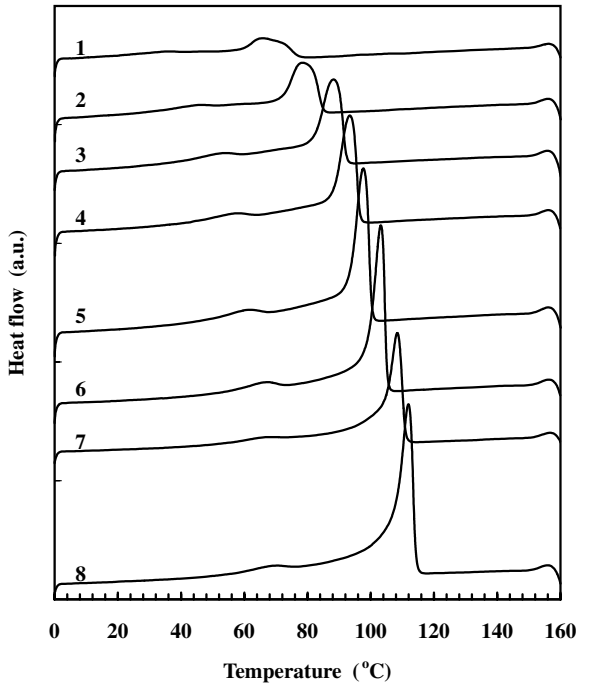

Fig. 10. Evolution of crystallization behavior for PTREF fractions for Ziegler–Natta copolymer; PTREF fractionation temperature for each fraction is the same as in Fig. 7.

The melting peak temperatures of PTREF fractions of the Ziegler–Natta and metallocene copolymers were plotted against the corresponding SCB contents in Fig. 9. The melting temperature of Ziegler–Natta copolymer fractions substantially declined with increasing SCB content from 4 to 34 branches per 1000 carbons. The metallocene fractions showed only a slight change in the melting temperature with changes in SCB content from 18 to 37 branches per 1000 carbons. It is noteworthy that for those fractions having similar SCB contents, the Ziegler–Natta samples had significantly higher melting temperatures than the fractions for the metallocene copolymer. For example, at the SCB content of 25 branches per 1000 carbons, the melting temperature of the Ziegler–Natta sample was 94°C, while that of the metallocene sample was 62°C. This difference diminished gradually toward high SCB content. This observation leads to the conclusion that the melting of 1-butene/ethylene copolymers depends not only on SCB on content but also on the SCB distribution.

DSC exotherms were recorded during cooling of the melted PTREF fractions. Fig. 10 shows the DSC exotherms of PTREF fractions for the Ziegler–Natta copolymer; the crystallization temperature of these PTREF fractions varied considerably with PTREF elution temperature. The low-temperature fractions crystallized at lower temperatures with a relatively broad crystallization peak. For the PTREF fractions with higher elution temperatures, the crystallization curve shifted toward higher temperatures and the crystallization peaks became sharper. These results are similar to the melting results for the same PTREF fractions.

The DSC exotherms of the PTREF fractions for the metallocene copolymer are shown in Fig. 11. All the five fractions had very similar crystallization temperature and crystallization peak regardless of PTREF elution temperature. This implies that the SCB content has little influence on the crystallization of PTREF fractions of metallocene copolymer; this observation is similar to that for the melting of the PTREF fractions of the metallocene polymer.

The crystallization peak temperatures of PTREF fractions of the Ziegler–Natta and metallocene copolymers were plotted against SCB contents in Fig. 12. The crystallization temperature of the PTREF fractions for Ziegler–Natta sample considerably decreased with increasing SCB content, while the metallocene fractions only showed slight change in crystallization temperature. For those fractions having similar SCB contents, the Ziegler–Natta fractions showed significantly higher crystallization temperatures than the metallocene ones. Again, this is a strong indication that the SCB distribution has a more significant effect on the crystallization of 1-butene/ethylene copolymers than SCB the content.

The enthalpy of fusion for PTREF fractions of the Ziegler–Natta and metallocene copolymers, calculated from the DSC endotherms and the mass of samples, is

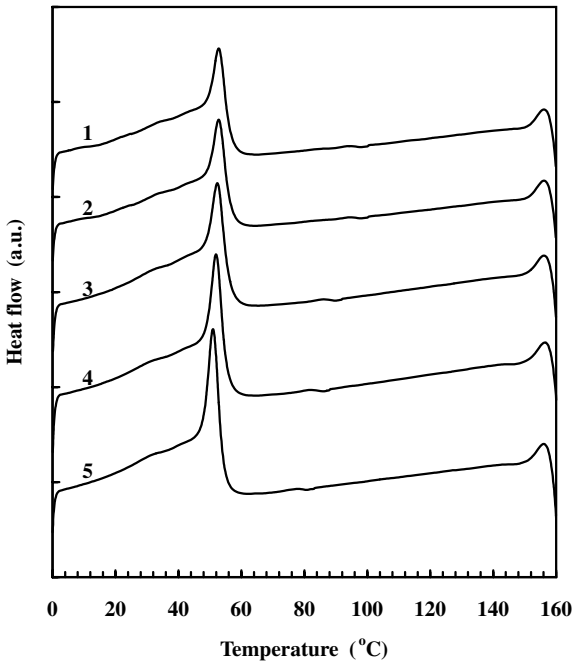

Fig. 11. Evolution of crystallization behavior for PTREF fractions for metallocene copolymer; PTREF fractionation temperature for each fraction is the same as in Fig. 8.

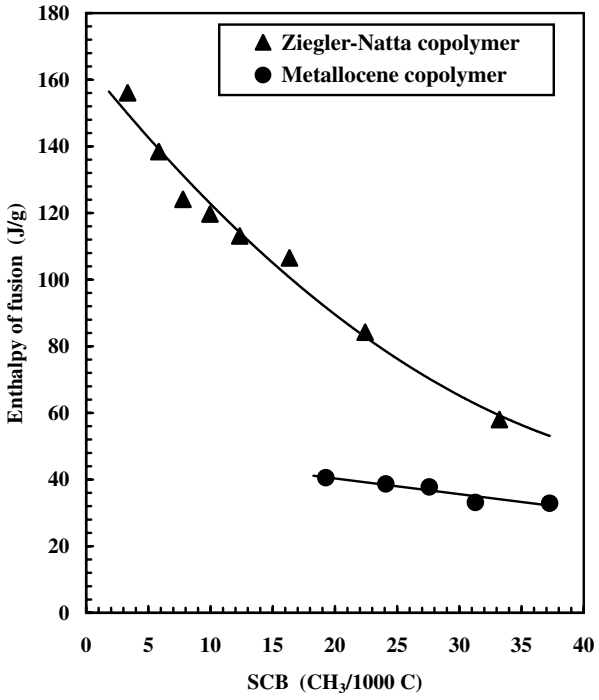

Fig. 13. Enthalpy of fusion as a function of SCB content for Ziegler–Natta and metallocene copolymers.

shown as a function of SCB content in Fig. 13. It is interesting to note that the enthalpy of fusion of the Ziegler–Natta sample declined substantially with increasing SCB content, whereas that of the metallocene sample only slightly decreased. Furthermore, the enthalpy of fusion of the Ziegler–Natta sample was much higher than that of the metallocene sample in SCB content range where the Ziegler–Natta and metallocene fractions had similar average SCB contents.

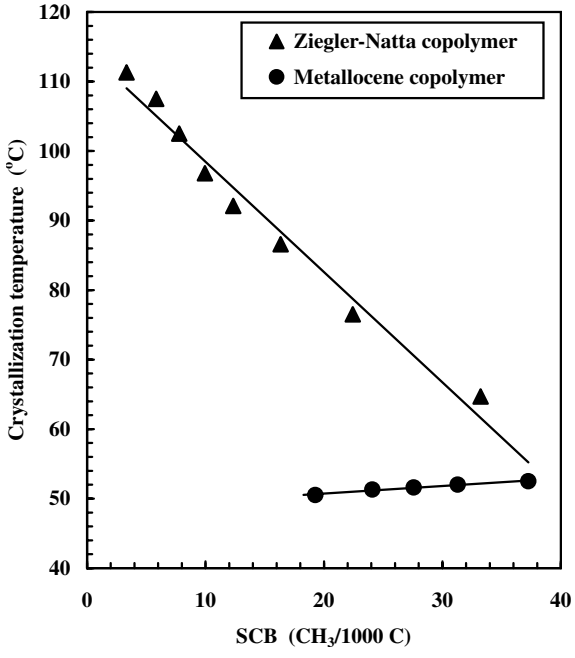

Fig. 12. Dependence of crystallization peak temperature on SCB content for Ziegler–Natta and metallocene copolymers.

The results presented above show that melting temperature, crystallization temperature, and enthalpy of fusion all depend heavily on SCB concentration for Ziegler–Natta copolymer. The value of all of these properties declined significantly with increasing SCB content, while the changes in these properties, as a function of SCB content was fairly small for the metallocene copolymer. Most importantly, for similar average SCB contents the PTREF fractions from the Ziegler–Natta sample had much higher melting temperatures, crystallization temperatures, and enthalpies of fusion than those of the metallocene sample. These results lead to the conclusion that the SCB or MSL distribution has a more significant effect than average SCB content on the melting and crystallization behaviors of 1-butene/ethylene copolymers. Similar observations, that the rheological behavior of ethylene/α-olefin copolymers depends more on the composition distribution than on the overall SCB content, have been reported recently [29]. This conclusion is also supported by our earlier observations that the MSL distributions of PTREF fractions for the Ziegler–Natta copolymer varied considerably with elution temperature, whereas those for metallocene copolymer possessed very similar MSL distributions [10].

The significant effect of SCB or MSL distribution on the melting and crystallization characteristics of ethylene/α-olefin copolymer can be better understood by comparing the SCB and MSL distributions of the Ziegler–Natta and

metallocene copolymers. As shown in Figs. 1 and 4, the Ziegler–Natta copolymer had a broad SCB distribution and a considerable amount of long MSLs. As pointed out earlier, the branches (except methyl) for polyethylene copolymers are excluded from crystals and the crystallization for the two copolymers is MSL-controlled. These long sequences can form stable and thick lamellar crystals under normal conditions [4,11]. With increasing PTREF elution temperature, the number of longer sequences increases considerably in PTREF fractions of the Ziegler–Natta copolymer [10]. As a result, the melting temperature, crystallization temperature, and enthalpy of fusion all increased with increasing MSL. The metallocene copolymer, as shown in Figs. 1 and 5, had a narrow SCB distribution and MSL distribution ranging from 18 to 37 carbons. The short sequences can only form metastable fringed-micellar type crystals which can be easily melted and can only be crystallized under favorable conditions [3,4,11]. Even if the TREF elution temperature for the metallocene copolymer is increased, the MSLs of PTREF fraction are still within the narrow sequence range. Thus, the melting temperature, crystallization temperature, and enthalpy of fusion are all not sensitive to SCB content (see Figs. 9, 12, and 13).

4. Conclusions

ATREF analysis showed that the Ziegler–Natta copolymer had a broad bimodal SCB distribution, while the metallocene copolymer showed a much narrow SCB distribution. SNA-DSC analysis revealed that the Ziegler–Natta copolymer possessed a broad MSL distribution with significant amount of long methylene sequences. In contrast, the metallocene copolymer showed a much narrower MSL distribution and contained a large amount of short methylene sequence.

The difference in the SCB and MSL distributions resulted in a marked difference in the melting and crystallization characteristics of PTREF fractions for the two polymers. The melting temperature, crystallization temperature, and enthalpy of fusion for PTREF fractions of the Ziegler–Natta sample decreased markedly with increasing SCB content, whereas these properties of the PTREF fractions for the metallocene sample only changed slightly. Furthermore, the PTREF fractions of the Ziegler–Natta copolymer had much higher melting temperatures, crystallization temperatures, and enthalpies of fusion than those of the metallocene copolymer with the same average SCB contents. This leads to the conclusion that the SCB distribution has a more significant effect on melting and crystallization behavior of 1-butene/ethylene copolymers than the SCB content.

Acknowledgements

The authors acknowledge the support of this work by the Natural Sciences and Engineering Research Council of Canada and NOVA Chemicals Corporation.

References

[1] Clas SD, McFaddin DC, Russell KE, Scammell-Bullock MV. J Polym Sci, Part A: Polym Chem 1987;25:3105–15.
[2] Mathot VBF, Pijpers MFJ. J Appl Polym Sci 1990;39:979–94.
[3] Peeters M, Goderis B, Vonk C, Reynaers H, Mathot V. J Polym Sci, Part B: Polym Phys 1997;35:2689–713.
[4] Peeters M, Goderis B, Reynaers H, Mathot V. J Polym Sci, Part B: Polym Phys 1999;37:83–100.
[5] Schouterden P, Groeninckx G, Van der Heijden B, Jansen F. Polymer 1987;28:2099–104.
[6] Wilfong DL, Knight GW. J Polym Sci, Part B: Polym Phys 1990;28:861–970.
[7] Defoor F, Groeninckx G, Schouterden P, Van der Heijden B. Polymer 1992;33:3878–83.
[8] Alamo RG, Viers BD, Mandelkern L. Macromolecules 1993;26:5740–7.
[9] Hosoda S. Polymer J 1988;20(5):383–97.
[10] Zhang M, Lynch DT, Wanke SE. J Appl Polym Sci 2000;75:960–7.
[11] Alizadeh A, Richardson L, Xu J, McCartney S, Marand H. Macromolecules 1999;32:6221–35.
[12] Adisson E, Ribeiro M, Deffieux A, Fontanille M. Polymer 1992;33(20):4337–42.
[13] Keating MY, McCord EE. Thermochim Acta 1994;243:129–45.
[14] Starch P. Polym Int 1996;40:111–22.
[15] Fu Q, Chiu FC, McCreight KW, Guo M, Tseng WW, Cheng SZD, Keating MY, Hsieh ET, DesLauriers PJ. J Macromol Sci Phys 1997;B36(1):41–60.
[16] Keating M, Lee I, Wong CS. Thermochim Acta 1996;284:47–56.
[17] Stack GM, Mandelkern L. Macromolecules 1988;21:510–4.
[18] Ungar G, Keller A. Polymer 1987;28:1899–907.
[19] Bonner JG, Frye CJ, Capaccio G. Polymer 1993;34:3532–4.
[20] Muller AJ, Hernandez ZH, Arnal ML, Sanchez JJ. J Polym Bull 1997;39:465–72.
[21] Zhang M. MSc thesis, University of Alberta, Edmonton, Canada, 1999.
[22] Kapoglanlan SA, Harrison IR. Thermochim Acta 1996;288:239–45.
[23] Zhou H, Wilkes GL. Polymer 1997;38(23):5735–47.
[24] Starck P. Polym Int 1996;40(2):111–22.
[25] Defoor F, Groeninckx G, Reynaers H, Schouterden P, Van der Heijden B. J Appl Polym Sci 1993;47:1839–48.
[26] Hsieh ET, Tso CC, Byers JO, Johnson TW, Fu Q, Cheng SZD. J Macromol Sci, Phys 1997;B36(5):615–28.
[27] Wild L. Adv Polym Sci 1991;98:1–47.
[28] Soares JBP, Hamielec AE. Polymer 1995;36:1639–54.
[29] Gelfer MY, Winter HH. Macromolecules 1999;32(26):8974–81.